Mechanisms of Latent Image Formation in Photothermographic Silver Imaging Media*

Chaofeng Zou and M. R. V. Sahyun†
Dry Imaging Technology Center, 3M, 3M Center, St. Paul, MN 55144

B. Levy†
Department of Chemistry, Boston University, Boston, MA 02215

N. Serpone
Department of Chemistry, Concordia University (SGW Campus), Montreal, Quebec H3G 1M8, Canada

The purpose of this paper is to establish that significant differences exist between mechanisms of latent image formation in conventional silver halide emulsions and in dry processed, photothermographic silver media. We develop our analysis in two ways: (1) through a review of salient literature; and (2) by highlighting areas of research that clearly delineate between conventional silver halide and photothermographic media, involving mathematical modeling, laser spectroscopy, and photocharge studies. We conclude that catalytic juxtaposition of a silver carboxylate phase with a silver halide phase leads to profound changes in the photophysics of the silver halide. Thus characteristically different latent-image-forming mechanisms prevail in thermally developed media, compared with conventional, negative-working silver halide photographic films, and transfer of technology from one to the other is not obvious.

Journal of Imaging Science and Technology 40: 94 – 103 (1996)

Introduction

Literature Review. Thermally processed, silver-based imaging media have been known since 1847.[1] Their practicality for imaging applications resulted from the discovery more than 25 years ago that the photosensitivity of films and papers based on thermally developable silver carboxylates could be drastically enhanced through incorporation of silver halide microcrystals.[2] The evolution of such photothermographic media into today's commercial products has been documented by Morgan[2b,c] and by Shepard.[3] The basic chemistry has been reviewed by Zavlin and co-workers[4] and by Klosterboer[5]; in the latter work, Klosterboer proposes an elementary, but quantitative, model of photothermographic response.

In all of this literature it has been tacitly assumed that the photochemistry of latent image formation in thermally processed silver halide–silver carboxylate systems is the same as in conventional gelatin-dispersed silver halide grains. The potential photophysical consequences of drastic alteration of the grain environment have been completely ignored. The literature further fails to resolve the related issue: whether or not in the thermally processable media the exposed silver halide grains themselves or only the image-forming silver carboxylate salt(s) are developed, i.e., whether or not the latent image responsible for thermal developability of photothermographic films also confers developability on the silver halide grains that capture light to initiate the latent-image-forming process. Zavlin et al.[4] and Klosterboer[5] disagree on this point. Morgan[2c] specifically states that the silver halide is not consumed in forming the silver image. Studies on temperature dependence of latent image formation[6] in conventionally processed and thermally developed films, however, support the idea that the conventional and photothermographic processes exhibit a mechanistic commonality .

If, as suggested, photolysis mechanisms in the photothermographic media are essentially the same as in conventional films, latent image formation should conform to one of the mechanisms usually proposed for it in the photographic literature. These include:

1. the Gurney–Mott model,[7a]
2. the Hamilton–Bayer model derived therefrom,[7b]
3. the concentration theory of Mitchell,[8]
4. the phase formation theory of Malinowski,[9] and
5. the "photographic diode" and "photographic transistor" models of Levy.[10]

All of these models have stimulated experiments leading to significant advances in photographic technology. At the same time, differences between points of view represented by these mechanistic proposals have not been unequivocally resolved, despite attempts to synthesize the principal features of these models into some sort of comprehensive scheme.[11] Following the benchmark lecture in 1979 by Malinowski, which critiqued the Gurney–Mott model and became the basis for Ref. 9, a large part of the photographic community has perceived the question of mechanism or, more appropriately, mechanisms of latent image formation in conventional silver halide media to be "open."

However, a body of experimental evidence suggests that this analogy to latent image formation in conventional silver halide emulsions may be wholly inappropriate. According to Shepard,[3] Morgan and coworkers have shown

Original manuscript received December 9, 1995. Revised January 19, 1996.

* Contribution No. 95-0409C from the Information, Imaging and Electronics Sector Laboratories, 3M.

† IS&T Fellow and Senior Member

that when a completely fogged (to surface development) silver halide emulsion is incorporated into a photothermographic construction, the resulting material exhibits normal sensitometry on thermal development, i.e., the D_{min} is comparable to that obtained with an unfogged emulsion. Subsequent to the initial work of Morgan and Shely,[2a] it has been shown that other light-absorbing, photosensitive materials can be substituted for the silver halide component in photothermographic silver carboxylate-based compositions and confer useful levels of sensitivity. These materials include zinc oxide,[3] titanium dioxide[12] and silver tetrahydrocarbylborate salts, $AgPh_4B$.[13]

It has also been claimed[14] that there is no correlation between the activity of spectral sensitizing dyes in photothermographic films and in conventional silver halide systems, and even that certain dyes allow the silver halide component to be completely eliminated from silver carboxylate photothermographic formulations.[15] Accordingly these dyes should enable photolysis of the silver carboxylate component itself, which implies that the system dye/silver carboxylate may comprise a photographic diode as defined by Levy.[10] (In this connection it is important to note that the photographic diode concept implies only that there are two phases in juxtaposition that can undergo ionic and/or electronic equilibration. The photographic diode concept does not imply that the interface between phases is epitaxial or that the resulting heterojunction has no barriers.)

Chemical sensitization is the key to high photographic sensitivity achieved by conventional gelatin silver halide emulsions. Thereby catalytic sites are formed on the silver halide grain surface, and/or the grains are doped to create centers that facilitate electron–hole separation after photoexcitation. Subsequently, according to some theories, these "sensitivity specks" localize the photoelectrons where the chemical effects of multiple absorbed quanta can be concentrated.[16,17] Given the large volume of literature on this subject in the context of conventional emulsion technology, e.g., as reviewed by Pitt et al.,[17] the paucity of literature describing chemical sensitization of grains for use in thermally developed silver carboxylate media is striking.

Recently Bolshakov and Goryaev[18] reported that sulfur (S) sensitization of emulsions used in phothermographic media leads only to high fog levels; the usual sensitivity centers are too active as development centers under conditions of thermal development. The same authors report that Au sensitization alone may yield 0.30–0.45 log E speed increases in photothermographic media. Such sensitivity enhancements are not usually obtained in conventional emulsions *without* concurrent S sensitization.[17] Gold alone, however, provides significant enhancement of sensitivity of photographic emulsions to high-energy radiation.[19] Faelens[20] has observed effective sensitization with Au alone in a reducing environment, on the basis of which he postulates that Au_n^0 centers comprise the real sensitivity specks formed even under conditions of Au and S sensitization. His point of view has recently been supported by EXAFS studies on the structure of "gold silver sulfide" products on (111) AgBr surfaces.[21] (These EXAFS experiments naturally required higher Au levels than those normally used for chemical sensitization.) The reciprocity behavior of photothermographic films sensitized with Au suggests that it may be effecting a form of reduction sensitization[18] in these materials as well. Conventional S sensitization has proven useful, however, in thermally developed silver film formulations that do not employ silver carboxylate as an image former.[22]

Recently a new line of investigation relating to latent image formation has been opened to probe the earliest events in the formation of zerovalent silver species photochemically or radiochemically. This work posits an analogy between radiochemically synthesized small metal aggregates and pseudometallic clusters capable of initiating physical development.[23] According to the view of Klosterboer,[5] the analogy to physical development may be particularly relevant to modeling the chemistry of photothermographic media. Pulse radiolysis can be used to generate a population of solvated electrons, which then reduce silver ions from some precursor in solution, leading eventually to autocatalytic growth of Ag_n^0 cluster species; the whole process is probed by time-resolved optical absorption spectroscopy.[24–27]

Such studies have now been extended to the silver salts of polyacrylic acid[26] and of gelatin[27] in solution as silver cluster precursors. In both these systems silver ion is present in the form of a silver carboxylate salt. This work demonstrates that latent-image-like Ag_n^0 clusters can form efficiently in silver carboxylates, at least in solution, and that concentration processes producing these species from the silver atoms formed by initial electron trapping occur in these media on the microsecond time scale. Accordingly, cluster growth involves a sequence of alternating ionic and electronic steps involving cationically charged intermediate clusters, with strong similarities to the Mitchell mechanism of latent image growth in silver halide,[28] as well as to the early proposals of Matejec.[29] A salient feature of this sequence is the key role of spectroscopically detectable Ag_2^+.[30] This cationic intermediate is generally thought to be unstable in conventional silver halide grains.[31] We propose that these studies may be relevant as models of latent-image-forming processes in silver carboxylate-based photothermographic media.

Purpose of the Study. We undertook the experiments and simulation studies described in this paper to provide points of comparison with the theories for latent image formation in conventional silver halide grains. Our objective was to establish a realistic conceptualization of latent image formation in photothermographic silver halide–silver carboxylate imaging media. Although we do not start with the heretofore standard presumption that these processes must be the same mechanistically, we do assume that in both cases the latent image species—which serves to nucleate direct or physical development in the case of conventional materials, or a physical development process in the photothermographic case[5]—is a silver cluster, smaller than threshold size for onset of metallic character, and, most likely, positively charged.[24,28–32] Our concerns here are the locus of its formation and the process by which it evolves in response to absorption of photons, presumably by the silver halide component of the photothermographic mixture.

We further assume that established interface phenomena provide a paradigm for description of the photochemistry of silver-based photothermographic media. In their simplest form, these media comprise a minimum of three solid components forming separate phases on a microscopic scale: polymeric binder, microcrystalline silver carboxylate salt(s), and silver halide. Three types of interface regions are thus possible: (1) silver halide–binder, (2) silver carboxylate–binder, and (3) silver halide–silver carboxylate. The patent literature[2b] specifically speaks of the spatial relationship between silver halide and silver carboxylate as "catalytic proximity" and "synergistic association." Furthermore, photothermographic systems have been described in which the silver halide is formed by the metathetical reaction of silver carboxylate and a

halidizing reagent[2–5] and in which the silver carboxylate is synthesized in the presence of the silver halide.[4,5,33] Either of these solid-state chemical processes will result in a silver halide–silver carboxylate interface, which may be different for the different modes of preparation.

On the other hand, systems that comprise simple admixtures of silver halide and silver carboxylate, which are not necessarily predisposed to form such an interface, have not been claimed as useful or are of no technological importance. These considerations suggest that the silver halide–silver carboxylate interface is of prime importance to photothermographic function. It is thus another purpose of this article to establish some key characteristics of this interface and to assess its role in facilitating latent image formation.

Experimental

Materials. Ag(I)Br emulsions, $AgI_{.05}Br_{.95}$ or $AgI_{.02}Br_{.98}$, were prepared by the usual double-jet technique with control of pAg to yield cubic grains of narrow particle-size distribution. Habit and size were established by scanning electron microscopy (SEM) and x-ray diffractometry. Films were cast from emulsions that had been S and Au sensitized to optimum, as monitored by wet testing; coating weights were ca. 3.0 g Ag/m^2.

These emulsions were also incorporated, unsensitized, into photothermographic formulations according to the procedure described by Winslow and Maw.[33a] At the conclusion of the silver carboxylate ("soap") synthesis, these formulations comprised (1) 9.3 mol % (based on total silver) of the emulsion containing 5 % I, or (2) 4.6 mol% of the 2% I emulsion. Commercial behenic acid, which is actually a mixture of fatty acids and has the composition reported by Klosterboer,[5] was used in this process. (The resulting soaps are designated "AgBeh.") The silver soap(s) incorporating Ag(I)Br were then dispersed by homogenization into polyvinylbutyral in ethanol. (Samples for laser flash spectroscopy were removed immediately after homogenization and diluted to 1×10^{-4} M Ag with spectroscopic-grade absolute ethanol.)

According to Winslow and Maw's procedure, additional halide is added subsequent to precipitation of silver behenate and after homogenization of the AgX–AgBeh admixture, in order to control the pAg of the dispersion. In this case $CaBr_2$ (0.04 M in methanol) was used in an amount equivalent to 2.5 mol% total silver. The particle diameter of the resulting in situ AgBr was ca. 0.006 μm by x-ray diffractometry,[34] too small for characterization of grain habit by SEM. In control experiments in which preformed emulsion was omitted, we demonstrated that this in situ AgBr contributed little to observable photosensitivity. After addition of reagents for thermal development[33a] the dispersion was coated on polyester film base to a weight of ca. 1.8 g Ag/m^2.

Preparations of both AgI[35] and AgBr[36] nanosols have been reported. The AgBr nanosol was synthesized in ethanol containing 0.5 wt% polyvinylalcohol (low molecular weight) as grain growth restrainer by sequential addition of volumes of 0.01 M tetraethylammonium bromide and 0.01 M $AgBF_4$, both in methanol, to give a final concentration of 1.0×10^{-4} M silver; the bromide salt was used in 10% excess to provide a pAg of ca. 9 during this process. AgBr particle size was estimated by x-ray diffractometry to be ca. 60 Å, comparable to that of the *in situ* AgBr in photothermographic films[2c]; sols were stable and exhibited no evidence of particle growth over several days in the dark.

Methods. Conventional films were developed after sensitometric exposure (Eastman Kodak Model 101 sensitometer) in a rapid x-ray developer. Characteristic curves were read by transmission densitometry, and speed, S, was assigned as the reciprocal of exposure required to yield an optical density of 0.6 over (base + fog). For these films the speed point falls at the low exposure end of the straight-line portion of the characteristic curve. Photothermographic films were similarly exposed and developed, using a heated roll developer for 15 s at 121°C; characteristic curves were read in the same manner as for the conventional films.

Time-resolved photocharge measurements (Dember effect) used instrumentation and data analysis methods previously described.[37] Samples were excited with a broadband Xe flash source (pulse width of 0.7 μs FWHM). Use of narrow bandpass filters showed that photocharge response was concentrated near 400 nm (intrinsic AgBr absorption). All measurements were made in air at room temperature under safelight conditions. Only data from the first flash exposure of each sample were used; previous exposure history has been shown to bias photocharge signals.[37c,38]

Laser flash photolysis, followed by transient absorption spectroscopy, was carried out, using instrumentation previously described[39] as adapted for the study of silver halide media.[35,40,41] Liquid dispersions in a 2-mm cell (volume = 0.6 mL) were exposed with a pulse (30 ps FWHM) from a frequency-tripled Nd:YAG laser at 355 nm focused to a 2-mm spot on the face of the sample cell. Laser pulse energies were reproducible to ±15%. The reported transient absorption spectra are computer averages of at least six experiments, all performed on the same sample. The sample was thoroughly mixed between experiments, and there was no indication of systematic variation of results with repeated exposure.

Results and Discussion

Model of Photothermographic Response. The Klosterboer–Rutledge model of photothermographic imaging media[5] assumes a *sphere of influence*: a volume (not necessarily spheroidal) of silver carboxylate surrounding each silver halide grain. Accordingly, if the grain is exposed, all the silver carboxylate in this sphere of influence is reduced to form image silver. The critical dimension of this sphere of influence may be determined by the diffusion range of silver ion from silver carboxylate to support the thermal physical development reaction. This model further assumes that only light absorbed by silver halide grains is actinic for latent image formation; it makes no assumptions about the mechanism of that process.

It follows that, optimally, there should be one silver halide grain for each of these reactive volumes in the coated layer. If there are fewer silver halide grains, then some silver carboxylate is undevelopable, even on exposure to D_{max}. If there is an excess of silver halide grains, then spheres of influence overlap and image-forming photons are wasted in redundant latent image formation.

Thus, if P is the number of photons that must be incident in a unit area of the photothermographic coating in order to develop to 50% of D_{max}, then

$$P = N \sum_n (x_n n t / f), \tag{1}$$

with the constraint $P \geq Nt/f$, where

- N = number of spheres of influence incorporating at least one silver halide grain per unit area,
- x_n = fractional number of those spheres of influence incorporating n silver halide grains,
- t = threshold number of photons that must be absorbed by one of those grains for it to have a 50% probability of latent image formation, and

f = fraction of that light incident on the sphere of influence (i.e., P/N) that is absorbed.

It can be assumed that f depends on grain size, d, as nd^3 for absorption in the intrinsic regime and as nd^2 in the spectral regime of dye sensitization.[42] It follows then that in the intrinsic region of the spectrum, f is independent of grain size to a first approximation. Because $\sum x_n = 1$ over the range $0 \le n \le \infty$, it also follows that, where N_o is the total areal density of spheres of influence (with or without silver halide grains) in the coating,

$$N = N_o \sum_n x_n = N_o(1 - x_0) \tag{2}$$

and

$$D_{\max} \alpha \sum_n x_n = (1 - x_0) \tag{2a}$$

over the range $1 \le n \le \infty$. We can estimate x_n for a Poisson distribution of grains among spheres of influence; thus

$$x_n = [\lambda^n \ \exp(-\lambda)]/n!, \tag{3}$$

where λ is the mean number of silver halide grains per sphere of influence in the coating, and where, for the case $n = 0$,

$$x_0 = \exp(-\lambda). \tag{3a}$$

The sum $\sum_n x_n = \lambda$, by definition, and $P = Nt\lambda/f$ for $\lambda \ge 1$, as required by the boundary condition.

For a sphere of influence of radius r,

$$\lambda = (4\pi m r^3/3d^3)[V_m(\text{AgBr})/V_m(\text{AgBeh})], \tag{4}$$

where m is the mole fraction AgBr in the AgBr–AgBeh admixture, and V_m is the molal volume of the indicated phase. On evaluation of the constants we obtain

$$\lambda = 0.30\, mr^3/d^3, \tag{4a}$$

and in Table I values of λ and $(1 - x_0)$ are given for various grain sizes, using $m = 0.093$ and $r = 0.4$ μm, consistent with previous estimates.[5]

Grain-size-dependent factors in photospeed according to this model are given by

$$f(d) = (N_0 t/f)(1 - x_0)/P. \tag{5}$$

The second factor in the numerator corrects for those spheres of influence that are inert owing to the absence of a silver halide grain. Using Eq. 5 we estimate $\log_{10}(\text{Speed}_{\text{rel}})$ as $\log_{10} f(d)$ in Table I. Absolute speeds require numerical evaluation of the factor $(N_0 t/f)$. In itself, however, $f(d)$ represents an upper limit measure of efficiency with which photons are utilized in latent-image formation in a photothermographic film.

TABLE I. Parameters of the Model of Photothermographic Response

d (μm)	λ	$(1 - x_0)$	$\log_{10}$ Speed$_{\text{rel}}$
0.035	4.2	0.985	–0.63
0.040	2.8	0.94	–0.47
0.045	1.96	0.86	–0.36
0.050	1.44	0.76	–0.28
0.055	1.07	0.66	–0.21
0.060	0.83 (1.0)*	0.56	–0.25
0.080	0.35 (1.0)*	0.30	–0.53

* Required by the boundary condition for use in estimating $f(d)$; see text.

TABLE II. Experimental Sensitometry of Photothermographic Films

d (μm)	$D_{\min}$	$D_{\max}$	$\log_{10}$ Speed
0.035	0.18	4.1	1.50
0.040	0.19	3.9	1.70
0.045	0.20	3.8	1.80
0.050	0.20	3.8	1.90
0.055	0.22	3.6	1.90
0.060	0.22	3.3	1.80
0.080	0.27	3.0	1.70

Comparison with Experiment. Ag(I)Br grains (2 mol% I) were admixed at the 4.6 mol% level, as described, with AgBeh to make photothermographic films. These films were exposed and processed to give the sensitometric responses of Table II. This level of silver halide, comparable to levels reportedly[2–4] employed in commercial photothermographic films, was selected to encompass the range of λ of interest for demonstrating correspondence of model and experiment. Major trends of Table I are reproduced in the data of Table II:

1. $D_{\max}$ decreases monotonically with grain size.
2. Speed exhibits a relatively flat response, passing through a maximum near the grain-size level predicted by the model.

There is good linearity ($r = 0.932$) between estimated and observed speed values, as shown in Fig. 1. At the same time, $D_{\max}$ was expected to decrease more precipitously with d than was found experimentally. We might accordingly imagine an increase in covering power with increasing redundancy of nucleation of development ($\lambda > 1$) in the experimental films.

From comparison of model and experiment, we conclude: (1) that the corollary of the Klosterboer–Rutledge model,[5] namely, that optimum sensitivity requires one silver halide grain per silver carboxylate sphere of influence, is fundamentally valid, and (2) that usual grain size–speed

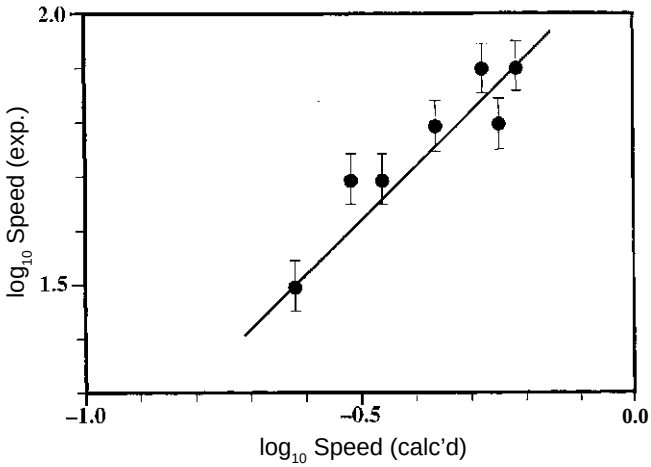

Figure 1. Correlation between intrinsic photospeeds ($\log_{10}$ scale) predicted by mathematical model of an Ag(I)Br–AgBeh photothermographic film and experimental results; Ag(I)Br grain size was variable in both calculations and experiment.

relationships from conventional silver halide technology[42] do not apply to such photothermographic systems.

The usual processes of admixture of silver halide and silver carboxylate materials, however, may be expected to yield a stochastic distribution of AgX grains among spheres of influence. Thus, according to Poisson statistics (Eq. 3), on average 2.3 grains of AgX per sphere of influence must be present in order to ensure that ≥90% of the spheres incorporate at least one AgX grain. This is a fundamental inefficiency of photothermographic silver media as usually constructed, requiring imaging exposures ca. 0.36 log E greater than ideal.

Photocharge Studies. Time-resolved photocharge studies, the so-called Dember photoeffect, have proven useful in clarifying latent-image-forming mechanisms in conventional silver halide emulsion systems.[16,37,38,43] We previously studied a series of cubic Ag(I)Br photoemulsions (5 mol% I) by this method, in which grain size over the regime ($0.055 \le d \le 0.45$) μm, was the principal variable.[44] We drew three salient conclusions:

1. Only chemically sensitized grains (S + Au) yielded a significant photocharge signal. We attribute this to inefficient electron–hole separation in the absence of sensitivity specks.
2. Positive photocharge signals imply that more light is absorbed at the backs (the sides away from incidence of exposing light) than at the fronts of individual grains.
3. The magnitude and duration of photocharge signals increase monotonically with increasing d.

This third observation suggests that mean ambipolar electron–hole separation distance, L, is determined by the depth of the depletion layer in individual grains. This is, in turn, limited by—but not necessarily equal to—one-half the linear grain dimension, d, not to exceed 0.1 μm.[45] Accordingly, neither electrons nor holes escape the grain, i.e., become transferred to an external medium, in these experiments.

These inferences were based on analysis of the data in accord with the equivalent circuit model of the photocharge experiment whereby the signal, V_D, is given as

$$V_D = -2.303\ \Phi I A(4\pi L/\varepsilon), \qquad (6)$$

in which

I = exposure (photons/cm^2),
A = fraction of actinic light absorbed,
Φ = quantum efficiency for formation of free electrons and holes, and
ε = the static dielectric constant of the silver halide grains.

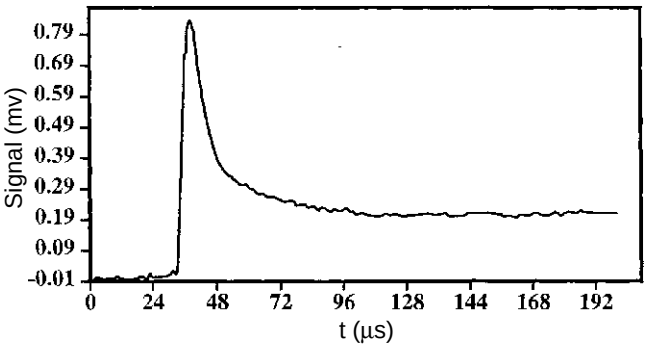

Figure 2. Representative oscillograph trace illustrating time-resolved photocharge signal resulting from flash exposure of a photothermographic film (d = 0.045 μm).

TABLE III. Photocharge Responses, V_D, of Photothermographic Films; Comparison with Light-Absorption-Corrected Responses, V_{corr}, for Conventional Films

d (μm)	V_D (mV)	V_{corr} (mV)
0.055	200	0
0.075	150	+87
0.10	150	220
0.22	265	870
0.45	265	670
Average	(206±50)	—

Because exciton–sensitivity speck interaction leads to highly efficient electron–hole separation, Φ = ca. 1 for the chemically sensitized emulsions. Thus, in these chemically sensitized grains in a gelatin environment, recombination losses are unimportant.[31a,46]

Using the same series of emulsions *without chemical sensitization* we made a series of AgBeh-based photothermographic films, in which the Ag(I)Br comprised 9.3 mol% total silver, and repeated the photocharge experiment. A representative time-resolved photocharge oscillograph trace is shown in Fig. 2. Absorption spectroscopy, corrected for scattering,[47] showed no significant variation in light absorption (ca. 30% at 400 nm) with d among the photothermographic films (as was assumed in deriving the model in the previous section of this report). The magnitudes of the photocharge signals are reported in Table III. All signals decayed with half-lives of ca. 6 μs, again independent of d.

Other salient features of these data are:

1. Positive photocharge signals indicate optical anisotropy similar to that of the conventional silver halide films, in which case it has been proposed[37c] that more light is absorbed at the backs than at the fronts of the individual grains.
2. The magnitude of the photocharge signal for even the smallest grains in photothermographic films is comparable to that of midsize grains in conventional films. For comparison, V_D data from the previous experiments[44] with chemically sensitized grains, normalized to 30% light absorption, are given as V_{corr} in Table III.

Because no photocharge signals were observed for the same chemically unsensitized grains in the gelatin films, we infer that *electron–hole separation must be much more efficient in the Ag(I)Br–AgBeh system than in the unsensitized Ag(I)Br grains in gelatin*. It is not necessarily more efficient than in chemically sensitized grains, however. It further follows that *in the case of photothermographic films* L *is independent of grain size*; otherwise V_D would show a grain-size dependence. Thus band bending internal to the grains is not relevant to electron–hole separation when they are juxtaposed to AgBeh, and efficient electron–hole separation is enabled by some other aspect of the system.

Both of these features of the data set can be rationalized if we assume that the Ag(I)Br–AgBeh interface corresponds to a heterojunction that creates a *photographic diode*.[10–16] This situation is analogous to that obtained in silver halide microcrystals with different halide phases, wherein the phase boundaries act like heterojunctions that localize electrons and holes in different regions of the crystal.[48] Accordingly, excitons in Ag(I)Br are dissociated at the interface and photoholes remain trapped in the Ag(I)Br grains; photoelectrons are trapped at the heterojunction,

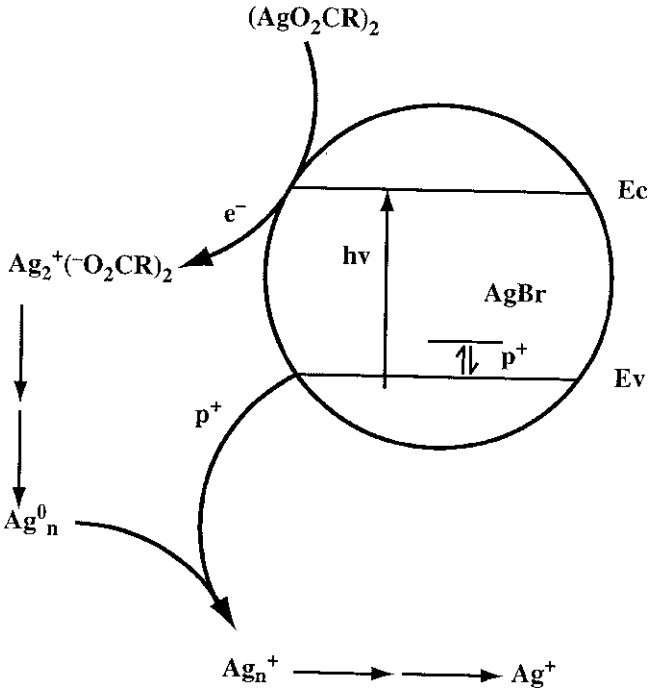

Figure 3. Schematic of photocatalytic mechanism for formation of a latent image at the AgBr–Ag carboxylate interface. Electron–hole pairs photogenerated in AgBr are separated at the interface; holes are trapped at I^- centers in AgBr; electrons are injected into the interfacial zone to reduce Ag^+ ions from Ag carboxylate, leading to stepwise formation of silver clusters, Ag_n^0; thermalized holes can reoxidize Ag^0 species to back to Ag^+.

even though it may not be barrierless. Thus Ag_n^0 cluster formation occurs by analogy to the chemistry observed in the pulse radiolysis studies of silver salts of polyacrylic acid[26] and gelatin[27] in solution. These materials show the strong ability of carboxylate anions to stabilize cationic silver clusters, Ag_n^{m+}, which we accordingly expect to form at the Ag(I)Br–Ag carboxylate interface.

We term this process the *photocatalytic mechanism*, because of its similarity to mechanisms delineated in other heterogeneous photocatalytic systems. The process is shown schematically in Fig. 3. At the interface between AgBr and Ag carboxylate phases, initially formed Ag^0 atoms grow into Ag_n^0 clusters capable of nucleating physical development.[5,23] Growth of similar clusters from Ag salts in solution (e.g., where initial Ag^0 atoms have been formed by capture of solvated electrons produced by pulse radiolysis[26,27]) provides a reasonable model of this process. Carboxylate anion stabilization[26] of intermediate cationic clusters, Ag_n^{m+}, may enable participation of intermediate species, e.g., Ag_2^+, which are not imputed to be important in conventional silver halide photochemistry. Ambipolar charge separation distance, L, in Eq. 6 is accordingly determined only by the width of the interfacial zone across which electron–hole separation occurs; it is thus independent of d, as observed. Carrier dynamics at the heterojunction lead to efficiency of electron–hole separation comparable to that achieved by exciton–sensitivity speck interaction in photographic grains in a conventional environment.

Laser Flash Photolyses. Laser flash photolysis of gelatin silver halide emulsions, monitored by transient absorption spectroscopy, has been reported by several groups.[41,49,50] Only in the work by the Serpone group,[41] however, have the results been resolved on the subnanosecond time scale, and hence they are amenable to kinetic analysis. We envisioned that extension of this methodology to the Ag(I)Br–AgBeh system could provide additional, convincing evidence in support of the picture developed to rationalize the above photocharge studies,. The photophysics and chemistry of the gelatin–silver halide emulsions may be strongly influenced by the gelatin–silver halide interface,[51] and cluster formation under conditions of laser flash photolysis in nanosize AgI has been shown to be a surface process.[52] Furthermore the grain size used in the previous studies was large compared with those normally used in photothermographic media.

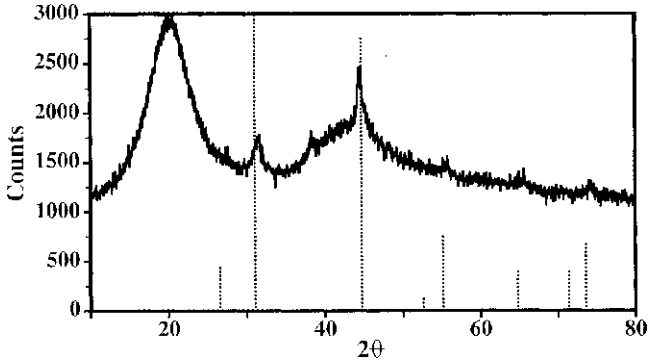

Figure 4. X-ray diffractogram[34] of a dried deposit of the AgBr nanosol used in laser flash photolysis experiments.

Therefore we chose a new model system for the AgBr component of photothermographic media, which comprised a polyvinylalcohol-dispersed AgBr nanosol in absolute ethanol. The x-ray diffractogram[34] of this nanosol, shown in Fig. 4, confirms crystalline (fcc) AgBr of grain size ca. 60 Å. This is about the same size as the AgBr grains found in some commercial photothermographic films, in which they are formed by in situ halidization of Ag carboxylate.[3] The absorption spectrum of the nanosol is shown in Fig. 5. We estimate the AgBr band edge by an Urbach's Rule analysis of the absorption edge as 435 nm, blue-shifted by 0.19 eV from the usual bulk value. According to the "particle-in-the-box" model,[53] this shift is consistent with a crystallite size estimate of ca. 60 Å provided by diffractometry.

Similar-sized AgI nanosols have been studied by the laser flash photolysis technique,[52] but we expect the photophysics of AgI and AgBr to be significantly different. The AgI is a direct band ionic semiconductor, as defined by Sturmer and Marchetti,[45] whereas the AgBr is an indirect band material.

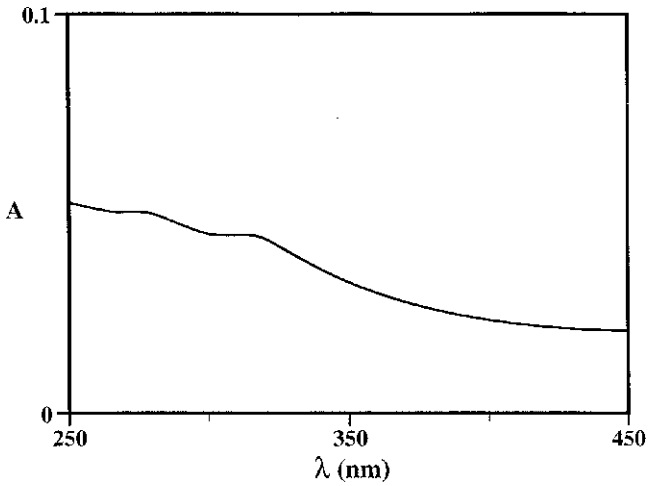

Figure 5. Absorption spectrum of AgBr nanosol.

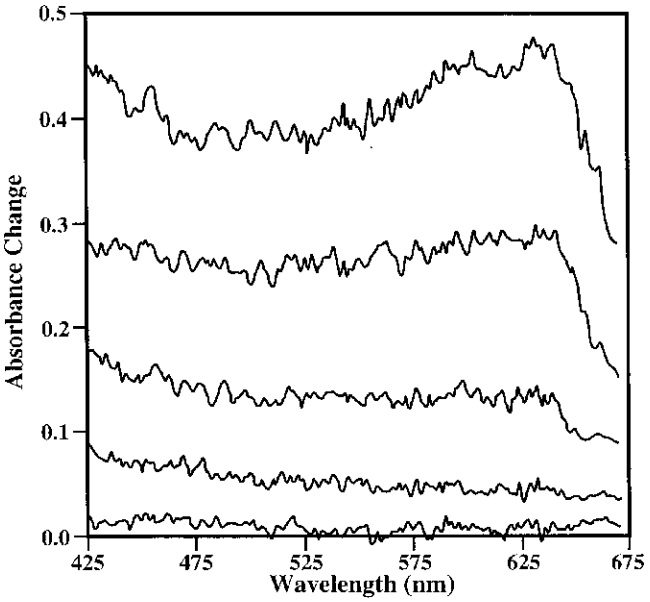

Figure 6. Absorption spectra of light-absorbing transients observed in the AgBr nanosol at various delay times (0.05, 0.2, 0.5, 1.0, and 2.0 ns, bottom to top of figure, respectively) following absorption of 355-nm laser pulse (30 ps FWHM).

Laser flash photolysis of the AgBr nanosol (30-ps pulse, 355 nm) led to the appearance of light-absorbing transients, as shown in Fig. 6. By analogy to the studies on photographic emulsions,[41,49,50] these transients are assigned to Ag^0 species of unknown nuclearity. Not all workers have accepted this assignment,[54] but a recent demonstration that small reduction sensitization, fog, and latent image Ag^0 clusters in emulsion grains[55a] all absorb in the visible regime of the spectrum is consistent with the assignment. Chemically produced silver(0) clusters on AgBr microcrystals typically exhibit absorption *maxima* in the 450- to 550-nm regime.[54]

As in the case of the conventional emulsion,[50] we associate growth of the transient(s) with time up to ca. 3 ns in the present system with increase in *number* of similarly sized clusters. This inference is based on the relative time invariance of the spectral distribution of absorption, which

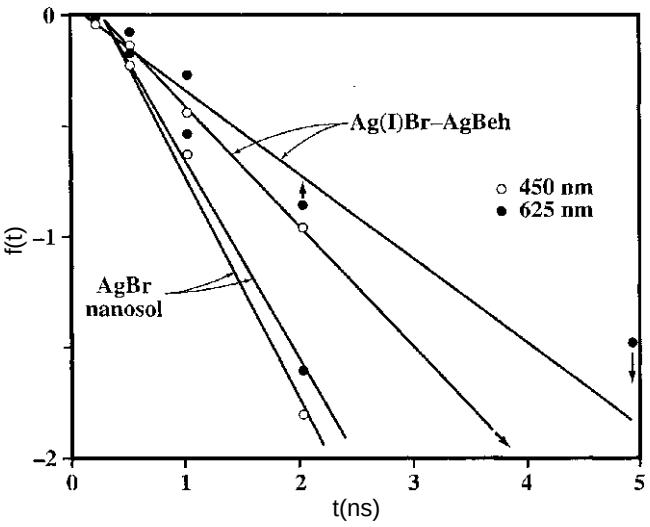

Figure 7. Pseudo-first-order analysis of data of Figs. 6 and 9 as $f(t) = \ln (1 - \Delta A/\Delta A_\infty)$ versus t (ns) for ΔA (absorbance change) at 450 and 625 nm.

TABLE IV. Kinetic Parameters: Laser Flash Photolysis of Ag Br Nanosol and Ag(I)Br–AgBeh Preformed Dispersion

	ΔA (AgBr nanosol)		ΔA [Ag(I)Br–AgBeh dispersion]	
	@ 450 nm	@ 625 nm	@ 450 nm	@ 625 nm
r*	0.992	0.991	0.999	0.980
k (ns^{-1})	(1.0 ± 0.1)	(0.9 ± 0.1)	(0.50 ± 0.01)	(0.37 ± 0.07)
t_i (ns)†	0.2	0.3	0.13	0

* Correlation coefficient.

† Induction period for onset of pseudo-first-order process.

should reflect cluster nuclearity and conformance of the process to pseudo-first-order kinetics (Fig. 7).

Parameters of the kinetic analysis are given in Table IV. Correspondence between this kinetic form and a process in which a number of Ag_n^0 particles evolve with time has been demonstrated by Huang et al.[56] in studies on base-catalyzed reduction of Ag^+ in isopropanol solution.

Laser pulse energy, I (mJ), dependence of the maximum observable transient, ΔA_∞, was analyzed as shown in the lower branch of Fig. 8, in which a plot of $\ln \Delta A_\infty$, measured at 500 nm, against ln I exhibits a slope of (2.4 ± 0.3), i.e., ca. 2. *From this result we infer biphotonic photolysis of this AgBr preparation.* Biphotonic photolysis may imply an Auger process[57] for photoelectron generation. Such a process requires involvement of either a donor or an acceptor center. Adventitious I^- can function in the former role.[50,58] There was no evidence of biphotonic dependence in photolyses of either AgI (direct gap) nanosols[35] or conventional gelatin-based Ag(I)Br photoemulsion,[41] although kinetic analysis of the rise and decay of photoluminescence provided evidence for operation of an Auger pathway for free-carrier generation in the latter case.[50]

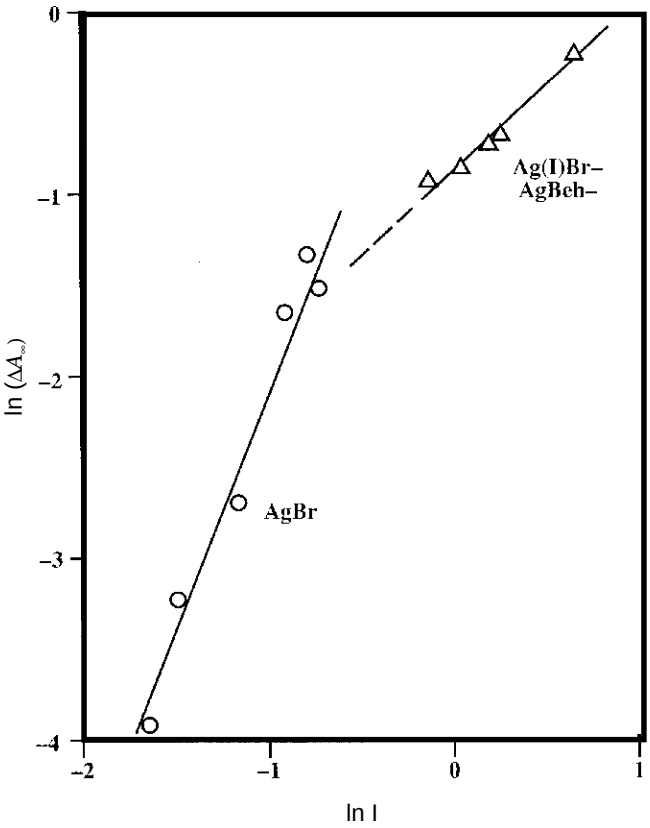

Figure 8. Dependence of $\ln \Delta A_\infty$ on laser pulse energy, ln I (mJ), for (a) AgBr nanosol and (b) AgBr–AgBeh dispersion.

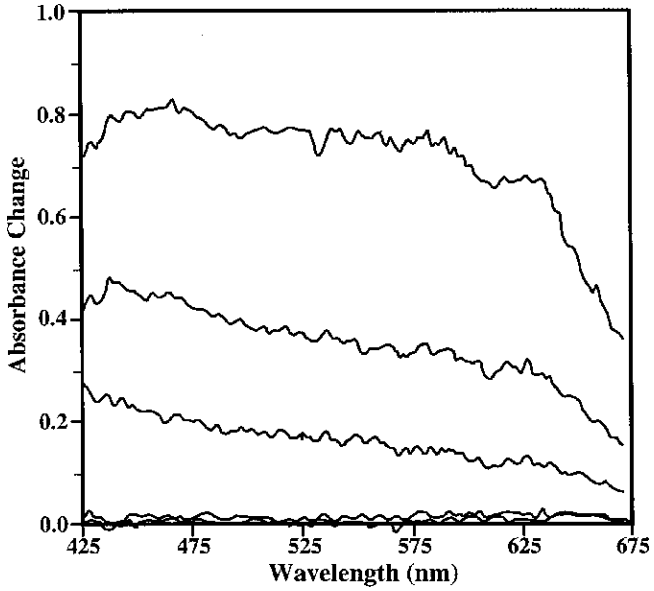

Figure 9. As in Fig. 6 for the AgBr–AgBeh system. Delay times are 0.2, 0.5, 1.0, 2.0, and 5.0 ns, bottom to top of figure, respectively.

The experiment was repeated with an ethanol-dispersed Ag(I)Br–AgBeh admixture (1×10^{-4} M in Ag). A control experiment with a halide-free AgBeh dispersion showed that the AgBeh was unresponsive at 355 nm in the absence of the silver halide component. Transient absorption spectra observed following 355-nm laser flash photolysis of the AgBr–AgBeh dispersion are shown in Fig. 9. This material yields a result qualitatively similar to that obtained with AgBr alone. The spectral distribution is, however, somewhat different from that observed with AgBr nanosol (Fig. 6) or Ag(I)Br photoemulsion.[41] The clearly defined existence of two maxima, one at $\lambda \leq 425$ nm and the other at $\lambda = 620$ nm in these spectra, suggests formation of two distinctly different kinds of Ag_n^0 species, either: (1) two distinct size distributions; or (2) two different environments. Observation of significantly different kinetic parameters for growth of absorption at the two median wavelengths (Table IV) supports either of these interpretations.

Formation of light-absorbing transients in this system is again completely reversible over the entire visible regime; the dispersion exhibits no change in light absorption by conventional spectrophotometry after ca. 50 laser shots. We infer that photoholes, probably localized at I^- centers in the Ag(I)Br grains,[58] are, on thermalization into the valence band, capable of reoxidizing Ag_n^0 photoproducts. This mechanism implies $E_{ox}(Ag_n^0) < E_v$ (AgBr), consistent with electrochemical potentials. In the presence of silver carboxylate the expected Borodin–Hunsdieker[59] reaction should lead to irreversible photochemistry:

$$\begin{aligned} &AgBr \xrightarrow{h\nu} Ag^0 + 1/2Br_2, \\ &Br_2 + RCO_2Ag \rightarrow RBr + AgBr + CO_2. \end{aligned} \qquad (7)$$

We accordingly assume that the chemistry of Eq. 7 does not obtain under the conditions of our experiments.

It is furthermore not energetically feasible for photoholes from the valence band of AgBr ($E_v = +1.05$ V vs SCE)[60] to oxidize carboxylate anion ($E_{ox} = +1.6 - 1.8$ V vs SCE)[61] directly. Accordingly, there is no mechanism for photohole injection into the "valence band" of AgBeh. Therefore reversibility of the laser photochemistry implies that these Ag_n^0 species must be within the interface zone in order to be accessible to photoholes from the valence band of AgBr. Separation of such silver(0) clusters in the interfacial region is an intuitively attractive concept. The entropy change accompanying formation of a new phase, i.e., silver(0), should be minimized in a region in which the Ag carboxylate lattice is already disordered to accommodate the interface with AgBr.

Obviously a fully reversible photochemistry cannot account for the formation of a stable latent image in a photothermographic silver film. We propose that the thermalized photoholes react preferentially with photogenerated Ag_n^0 species, as proposed above, but that other pathways must also exist for photohole removal. Thus:

(1) If Ag_n^0 formation occurs slowly with respect to the photohole thermalization lifetime (which may be on the time scale of microseconds to milliseconds[62]), such reactions may render the photochemistry irreversible.
(2) If, on the other hand, cluster nucleation and growth occur rapidly compared with the hole thermalization time, the photochemistry is completely reversible.

This interplay between clustering and hole detrapping dynamics leads to high intensity reciprocity failure (HIRF) in the photothermographic films. Short-duration, high-intensity exposures of conventional photographic emulsions are known to result in redundancy of latent image formation, hence photolysis to smaller silver(0) clusters.[63] Should this situation also occur in the photothermographic compositions, the greater susceptibility of smaller clusters to oxidative attack may also contribute to HIRF.

Data for laser pulse energy dependence of ΔA_∞ monitored at 500 nm (on the red tail of the shorter-wavelength-absorbing component in the transient absorption spectra) are also plotted in Fig. 8. These data are correlated by the upper branch of the plot. In this case the slope is 0.92, indicative of monophotonic photolysis. *Monophotonic photolysis of the Ag(I)Br–AgBeh system demonstrates that the same mechanism of electron–hole pair dissociation does not apply to nominally unsensitized AgBr (above) and to the Ag(I)Br–AgBeh system*. This inference supports a photocatalytic model, as proposed in connection with the photocharge effect studies. Accordingly, the interface is capable of dissociating excitons from silver halide to generate free electrons, which, in turn, reduce Ag^+. The AgBeh phase provides the reservoir of reducible Ag^+; formation of Ag_n^0 therein is consistent with the pulse radiolysis studies of Mostafavi and coworkers.[26]

Conclusions

A review of the literature on photothermographic silver halide–silver carboxylate imaging systems suggests that their photochemistry differs in several ways from what we should expect following the usual paradigms of silver halide photochemistry. We therefore undertook mathematical simulation and experiments involving conventional sensitometry, time-resolved photocharge measurements, and laser flash photolysis to clarify this issue.

From these studies we conclude that:

1. The usual relationships between grain size and photographic speed that characterize silver halide photography do not apply to the photothermographic media.
2. Chemical sensitization of silver halide grains is required for efficient electron–hole separation in

conventional silver halide emulsions, but not if the silver halide is interfaced with silver carboxylate.
3. Photoelectron–hole ambipolar separation distance is limited by grain size in gelatin–silver halide emulsion grains but not in the photothermographic environment.
4. Laser flash photolysis of AgBr at 355 nm proceeds by a biphotonic pathway; photolysis of the silver halide–silver carboxylate system under the same conditions is monophotonic.

We propose that the best model for the process of latent image formation in photothermographic silver halide–silver carboxylate imaging media derives from heterogeneous photocatalysis.[64] Accordingly, the silver halide in the admixture is a photocatalyst for interfacial reduction of Ag^+ from the silver carboxylate phase. This mechanism is feasible insofar as the silver halide–silver carboxylate heterojunction comprises a photographic diode,[10,16] but we emphasize that the heterojunction in this case is neither necessarily epitaxial nor without barrier.

Heterogeneous photocatalytic schemes for reduction of Ag^+ at, e.g., TiO_2 and ZnO, are well known,[65,66] although they usually involve reduction of Ag^+ ion from solution. They have been the basis for imaging systems involving printout or solution physical development.[66] Thus, silver halide can be substituted with other photocatalysts, e.g., $AgPh_4B$ and TiO_2, to form photothermographic constructions, even though the bottom of the conduction band for TiO_2 lies well below that for silver bromide[64b] (and, presumably, for Ag carboxylate).

Thus the photochemistry of image recording in photothermographic silver imaging media has little in common with the latent-image-forming processes in conventional photography, as usually envisioned according to the Gurney–Mott,[7a] Hamilton–Bayer,[7b] or Mitchell[8] paradigms. Furthermore, to the extent that conventional latent image formation, i.e., photolytic silver cluster formation away from the Ag carboxylate interface, occurs in the silver halide grains of a photothermographic film concurrent with the photocatalytic process described above, it may compete with the formation of a thermally developable latent image and, as a result, be counterproductive from an imaging point of view. ▲

Acknowledgment. We thank Prof. J. W. Mitchell, University of Virginia, for helpful discussions concerning mechanisms of latent image formation in conventional silver halide media, and we thank Dr. William Bernett and Mr. John Winslow of the Dry Imaging Technology Center, 3M, as well as Dr. Duncan McL. A. Grieve, Minnesota 3M Research, Ltd., Harlow, Essex, UK, for helpful discussions on the chemistry of photothermographic imaging media. We also thank Dr. David Whitcomb for his assistance with the Russian literature on this topic. We thank Ms. Susan Hill (St. Paul), Dr. Tongguang Zhang (Boston), and Prof. Devendra K. Sharma and Mr. Reza Danesh (Montréal) for their able technical assistance with the various experiments. Work in Montréal at the Canadian Centre for Fast Laser Spectroscopy was supported in part by 3M Canada, Inc., and in part by a grant from NSERC Canada. Dr. Myles Brostrom of the 3M Analytical and Properties Research Laboratory performed the x-ray diffraction analyses. Absorption spectroscopy of photothermographic films was carried out by Dr. M. E. Mueller, 3M Analytical and Properties Research Laboratory, following the methodology described in Refs. 44 and 47.

References

1. W. H. Fox Talbot, US Patent 5,171 (1847).
2. (a) D. A. Morgan and B. L. Shely, US Patent 3,457,075 (1969); (b) D. A. Morgan, *J. Imaging Technol.* **13**: 4 (1987); (c) D. A. Morgan, *Proc. SPIE* **1253**: 239 (1990).
3. J. W. Shepard, *J. Appl. Photogr. Eng.* **8**: 210 (1982).
4. P. M. Zavlin, A. N. Dyakonov, S. S. Mnatsakanov, S. S. Tibilov, P. Z. Velinzon, and S. T. Gaft, *Tekh. Kino. Telev., Nauka i Tekhnike* 9 (1990).
5. D. H. Klosterboer, in *Imaging Materials and Processes*, 8th ed., J. M. Sturge, V. Walworth, and A. Shepp, Eds., Van Nostrand-Reinhold, New York, 1989, Chap. 9.
6. T. E. Kekhva, V. N. Lebedev, and I. V. Sokolova, *Zhur. Fiz. Khim.* **65**: 2036 (1991).
7. (a) R. W. Gurney and N. F. Mott, *Proc. Roy. Soc. London* **A164**: 151 (1938); (b) B. E. Bayer and J. F. Hamilton, *J. Opt. Soc. Am.* **55**: 439 (1965); for a quantitative expression of this model see R. K. Hailstone and J. F. Hamilton, *J. Imaging Sci.* **29**: 125 (1985) and references cited therein.
8. J. W. Mitchell, *J. Photogr. Sci.* **31**: 148 (1983) and references cited therein, especially J. W. Mitchell, *Sci. Ind. Phot.* **28**: 493 (1957).
9. J. Malinowski, in *Growth and Properties of Metal Clusters*, J. Bourdon, Ed., Elsevier, Amsterdam, 1980, pp. 303ff.
10. B. Levy, *Photogr. Sci. Eng.* **27**: 204 (1983) and references cited therein.
11. G. Buerge, *Photogr. Sci. Eng.* **27**: 31 (1983).
12. J. J. A. Robillard, French Patent 2,254,047 (1973).
13. M. R. V. Sahyun, R. C. Patel, and R. Muthyala, US Patent 5,260,180 (1993).
14. I. H. Leubner, *Res. Discl.* **152**: 61 (Dec. 1976).
15. A. von Koenig, H. Kampfer, E. M. Brinckmann, and F. C. Heugebaert, US Patent 3,933,507 (1976).
16. (a) B. Levy, in *Photochemical Storage and Conversion of Energy*, E. Pelizzetti and M. Schiavello, Eds., Kluwer, Amsterdam, 1991; pp. 337ff; see also Ref. 10; (b) B. Levy, *J. Soc. Photogr. Sci. Technol. Japan* **54**: 477 (1991).
17. D. A. Pitt, M. L. Rachu, and M. R. V. Sahyun, *Photogr. Sci. Eng.* **25**: 57 (1981), and references cited therein.
18. (a) V. N. Bolshakov and M. A. Goryaev, *Opt. Tekh. Prom.* **11**: 68 (1991); (b) M. A. Goryaev, T. B. Kolesova, M. I. Timokhina, and I. M. Gulkova, in *Proceedings: Technology and Properties of Information Recording M aterials*, Moscow, 1992, pp. 67ff.; (c) M. A. Goryaev, in ICPS 1994: *Physics and Chemistry of Imaging Systems*, Vol. I, IS&T, Springfield, VA, 1994; p. 360 and references cited therein.
19. H. Hoerlin and F. W. H. Mueller, *J. Opt. Soc. Am.* **40**: 246 (1950).
20. P. Faelens, *J. Photogr. Sci.* **26**: 144 (1978); see also A. Hautot and H. Sauvenier, *Sci. Ind. Phot.* **28**: 57 (1957).
21. T. Murata, S. Emura, T. Nakayama, H. Takada, N. Tsuchiya, H. Maeda, and M. Nomura, in Ref. 18c, p. 100.
22. S. Goto, K. Okauchi, J. Kohno, and M. Iwagaki, US Patent 5,064,753 (1991); Japan Patent 86,137,147 (1986).
23. J. S. Yudelson, in Ref. 9, pp. 321ff.
24. M. Mostafavi, J. L. Marignier, J. Amblard, and J. Belloni, *Radiat. Phys. Chem.* **34**: 605 (1989); J. Belloni, M. Mostafavi, J. L. Marignier, and J. Amblard, *J. Imaging Sci.* **35**: 68 (1991).
25. A. Henglein, *Chem. Phys. Lett.* **154**: 473 (1989).
26. M. Mostafavi, M. O. Delcourt, N. Keghouche, and G. Picq, *Radiat. Phys. Chem.* **40**: 445 (1992); M. Mostafavi, M. O. Delcourt and G. Picq, *ibid.* **41**: 453 (1993); S. Remita, J. M. Orts, J. M. Feliu, M. Mostafavi, and M. O. Delcourt, *Chem. Phys. Lett.* **218**: 115 (1994).
27. (a) S. Kapoor, D. Lawless, P. Kennepohl, D. Meisel, and N. Serpone, *Langmuir*, **10**:3018 (1994); (b) for a preliminary account of this work see Ref. 18c, pp. 57ff.
28. J. W. Mitchell, *J. Imaging Sci.* **34**: 113 (1990).
29. R. Matejec, *Z. Phys.* **148**: 454 (1957).
30. R. Tausch-Treml, A. Henglein, and J. Lilie, *Ber. Bunsenges. Phys. Chem.* **82**: 1335 (1978).
31. (a) J. W. Mitchell, *J. Imaging Sci.* **35**: 341 (1991) and references cited therein; (b) M. R. V. Sahyun, in Ref. 9, pp. 379ff.
32. H. Hamano and J. Arai, *J. Photogr. Sci.* **27**: 17 (1979).
33. (a) J. M. Winslow and I. R. Maw, US Patent 4,161,408 (1979); (b) H. W. Altland and D. D. F. Shiao, US Patent 4,351,896 (1982).; (c) M. Simons, US Patent 3,839,049 (1972); (d) K. A. Penfound, US Patent 4,476,220 (1984).
34. AgBr crystallite size was estimated from line broadening in the diffractogram (Fig. 4) according to the Scherrer equation as described by H. P. Klug and L. E. Alexander, *X-Ray Diffraction Procedures*, John Wiley & Sons, New York, 1954.
35. O. I. Micic, M. Meglic, D. Lawless, D. K. Sharma, and N. Serpone, *Langmuir* **6**: 487 (1990).
36. K. P. Johansson, G. McLendon, and A. P. Marchetti, *Chem. Phys. Lett.* **179**: 321 (1991).
37. (a) B. Levy, *Photogr. Sci. Eng.* **15**: 279 (1971); (b) B. Levy, M. Lindsey, and C. R. Dickson, *ibid.* **17**: 115 (1973); (c) C. R. Dickson and B. Levy, *ibid.* **18**: 524 (1974); (d) K. C. Chang, F. P. Chen, and B. Levy, *ibid.* **24**: 55 (1980); **25**: 138 (1981).
38. H. Hada, M. Kawasaki, and T. Yoshida, *Photogr. Sci. Eng.* **25**: 201 (1981).
39. N. Serpone, D. K. Sharma, J. Moser, and M. Graetzel, *Chem. Phys. Lett.* **136**: 47 (1987), and references cited therein.

40. M. R. V. Sahyun, N. Serpone and D. K. Sharma, *J. Imaging Sci. Technol.* **37**: 261 (1993).
41. N. Serpone, D. Lawless, B. Lenet, and M. R. V. Sahyun, *J. Imaging Sci. Technol.* **37**: 517 (1993).
42. (a) G. C. Farnell, in *The Theory of the Photographic Process*, 3rd ed., T. H. James, Ed., Macmillan, New York, 1966, pp. 75ff.; (b) G. C. Farnell and J. B. Chanter, *J. Photogr. Sci.* **9**: 73 (1961).
43. (a) A. M. Kahan, *Photogr. Sci. Eng.* **21**: 237 (1977); (b) T. He, Z. Zhanghua, and W. Sue, *J. Photogr. Sci.* **36**: 189 (1988).
44. C. Zou, M. R. V. Sahyun, M. E. Mueller, B. Levy, and T. Zhang, *J. Imaging Sci. Technol.* **39**: 106 (1995).
45. D. M. Sturmer and A. Marchetti, in Ref. 5, p. 88.
46. L. Dünkel, E. Nutsch, and B. Kutschan, *Cybernetics Sys.* **24**: 281 (1993); see also Ref. 18c, p. 294.
47. B. Levy and N. Matucci, *Photogr. Sci. Eng.* **14**: 394 (1970).
48. Th. Müssig and G. Hegenbart, in *The International East-West Symposium III: New Frontiers in Silver Halide Imaging*, IS&T, Springfield, VA, 1992; see also discussion by R. K. Hailstone and D. E. Erdtmann, *J. Appl. Phys.* **76**: 4184 (1994).
49. A. K. Chibisov, G. V. Zakharova, and V. M. Belous, *Sci. Appl. Phot.* **35**: 386 (1994).
50. N. Serpone, D. Lawless, and M. R. V. Sahyun, *Supramolecular Chem.*, **5**: 15 (1995).
51. F. Evva, in *Proc. 5th Intl. Assoc. Gelatin Conf., 1988* IAG, Fribourg (CH), 1989; pp. 293, 299 and 304ff.
52. N. M. Dimitrijevic, M. I. Comor, and O. I. Micic, in *Symposium on Electronic and Ionic Properties of Silver Halides*, B. Levy, Ed., IS&T, Springfield, VA, 1991; p. 226ff.
53. N. Chestnoy, T. D. Harris, and L. E. Brus, *J. Phys. Chem.* **90**: 3393 (1986).
54. S. V. Patsera and B. T. Plachenov, *Zhur. Fiz. Khim.* **65**: 1441 (1991).
55. (a) T. Tani and M. Murofushi, *J. Imaging Sci. Technol.* **38**: 1 (1994); (b) S. Guo, M. Sc. Thesis, Rochester Institute of Technology, Rochester NY, October 1995.
56. Z. Y. Huang, G. Mills, and B. Hajek, *J. Phys. Chem.* **97**: 11542 (1993).
57. J. W. Mitchell, *J. Imaging Sci.* **34**: 5A, 217 (1990).
58. S. S. Tibilov, V. N. Lebedev, and S. V. Patsera, in Ref. 18c; p. 268. We thank Prof. Tibilov for communication of his results in advance of publication.
59. D. J. Cram and G. S. Hammond, *Organic Chemistry*, McGraw-Hill, New York, 1959; p.256.
60. (a) P. B. Gilman, Jr., *Pure and Appl. Chem.* **49**: 357 (1977); (b) I. H. Leubner, *Photogr. Sci. Eng.* **24**: 138 (1980) and references cited therein.
61. D. H. Geske, *J. Electroanal. Chem.* **1**: 502 (1959/60); B. Kraeutler and A. J. Bard, *J. Amer. Chem. Soc.* **99**: 7729 (1977).
62. M. Kawasaki, S. Hiraoka, and H. Hada, *J. Imaging Sci. Technol.* **36**: 525 (1992).
63. R. K. Hailstone, N. B. Liebert, M. Levy, and J. F. Hamilton, *J. Imaging Sci.* **31**: 255 (1987).
64. (a) M. Graetzel, in *Photocatalysis: Fundamentals and Applications*, N. Serpone and E. Pelizzetti, Eds., John Wiley, New York, 1989; pp. 123ff.; (b) T. Sakata, *ibid.*; pp. 311ff; (c) H. Arakawa, *TECHNO Japan* **18** (11): 10 (1985).
65. A. Fujishima and K. Honda, *Nature* **238**: 37 (1972).
66. (a) H. Jonker, C. J. Kippel, H. J. Hutman, J. G. F. Janssen, and L. K. H. van Beek, *Photogr. Sci. Eng.* **13**: 1 (1969); (b) E. Berman, *ibid.* **13**: 50 (1969); G. L. McLeod, *ibid.*, **13**: 93 (1969); (c) H. Tabei and S. Nara, Japan Patent 73,114,370 (1973); (d) Y. Yonezawa, Y. Momoki, H. Tanemura, and H. Hada, *Nippon Shashin Gakkaishi* **45**: 91 (1982); H. Hada, H. Tanemura, and Y. Yonezawa, *Nippon Kagaku Kaishi* **299** (1984); (e) B. Ohtani, Y. Okagawa, S.-I. Nishimoto, and T. Kagiya, *J. Phys. Chem.* **91**: 3550 (1987); J.-M. Herrmann, J. Disdier, and P. Pichat, *J. Catal.* **113**: 72 (1988); B. Ohtani, S. Zhang, J. Handa, H. Kajiwara, S.-I. Nishimoto, and T. Kagiya, *J. Photochem. Photobiol. A: Chem.* **64**: 223 (1992).